

# Cooperative coupling of ultracold atoms and surface plasmons

Christian Stehle, Claus Zimmermann, and Sebastian Slama\*

*Physikalisches Institut and Center for Collective Quantum Phenomena in LISA+,  
Universität Tübingen, Auf der Morgenstelle 14, D-72076 Tübingen, Germany*

(Dated: July 14, 2018)

Cooperative coupling between individual optical emitters and specific light modes is one of the outstanding goals in quantum technology. It is both fundamentally interesting for the extraordinary radiation properties of the participating emitters and has many potential applications in photonics. While this goal has been achieved using high-finesse optical cavities, cavity-free approaches that are broadband and easy to build have attracted much attention recently. Here we demonstrate cooperative coupling of ultracold atoms with surface plasmons that propagate on a plane gold surface. The atoms are excited by an external laser pulse, while surface plasmons are detected via leakage radiation into the substrate of the gold layer. With a maximum Purcell enhancement of  $\eta_{P,\max} = 3.1$  we deduce that a number of  $N \approx 100$  atoms are coupled with high cooperativity to surface plasmons.

PACS numbers:

It is a long-sought goal of photonics to gain ultimate control over light-matter interactions on the single photon level [1]. This goal is mainly motivated by the prospect of many possible applications, e.g. generation of single photons on-demand [2–4], control of the emission rate of quantum emitters [5], nonlinearities on the single photon level [6–8] and the construction of single photon switches [9] and transistors [10, 11]. All of these applications require high cooperativity, a regime of cavity quantum electrodynamics (cqed) in which an optical emitter radiates with high probability into a distinct light mode [15]. This regime is characterized by the condition that the cooperativity parameter  $\eta = 4g^2/(\gamma\kappa) > 1$ , with coupling constant  $g$ , natural line width of the emitter  $\gamma$  and decay rate of the light field amplitude  $\kappa$ . Please note that this regime is contained in the strong coupling regime of cqed in which  $g > \gamma, \kappa$ . The coupling constant  $g$  is proportional to the dipole moment  $d$  of the emitter and to the electric field  $\mathcal{E}_1$  connected to a single photon. High cooperativity can thus be reached by combining highly polarizable emitters with systems with large field enhancement. The latter condition can be reached e.g. in high-Q nanocavities with small mode volume [13, 14]. An even stronger concentration of optical fields is possible with surface plasmons (SP) [16–18]. While direct energy transfer from molecules to surface plasmons has been observed in early experiments [19, 20], the interaction of single photon emitters and surface plasmons has attracted renewed interest in the last years [21, 22]. In this context modified emission rates were measured [23–25], single plasmons were excited [26, 27], and strong coupling between excitons and surface plasmons was demonstrated [28–35].

(i.e. molecules, nanocrystals and quantum dots) are deposited as quantum emitters on the surface, proposals for trapping real ultracold atoms close to plasmonic structures have attracted much attention recently [36–38]. These proposals are based on the concept of dipole traps which are generated above plasmonic nanostructures, similar to the optical trapping of nanoobjects in plasmonically patterned light fields [39]. Real atoms have the advantage of being identical quantum emitters and having very narrow optical transitions with typical widths in the MHz range. Using quantum optics techniques clouds of atoms can be cooled to quantum degeneracy at temperatures on the order of nanokelvin [40]. They can be trapped with ultrahigh precision in magnetic micotraps [41] and in optical dipole traps [42] where they suffer very low intrinsic decoherence [43]. Plasmonic traps might even further improve the control over the motion of atoms in the subwavelength regime, with dramatic consequences for interatomic scattering properties within one trap and atomic tunneling rates between neighboring traps [38]. These traps could even be used for engineering strong p-wave interactions and the realization of exotic quantum many-body states with topological properties [44]. Moreover, atoms which are positioned very close to plasmonic structures couple with high efficiency to surface plasmon modes which could be used for single photon applications and for enabling long-range interactions between atoms [36, 38]. Please note that strong coupling is also pursued by combining cold atoms with nanophotonic waveguides [45, 61].

While in the above mentioned work artificial atoms

Despite the mentioned theoretical proposals only little experimental work has so far combined cold atoms with surface plasmons. In early work atoms have been reflected from evanescent light fields which were enhanced by surface plasmons on planar surfaces [47–49]. Recently, we could show experimentally that potential landscapes for ultracold atoms can be tailored by plasmonic microstructures with the prospect of

---

\*Electronic address: sebastian.slama@uni-tuebingen.de

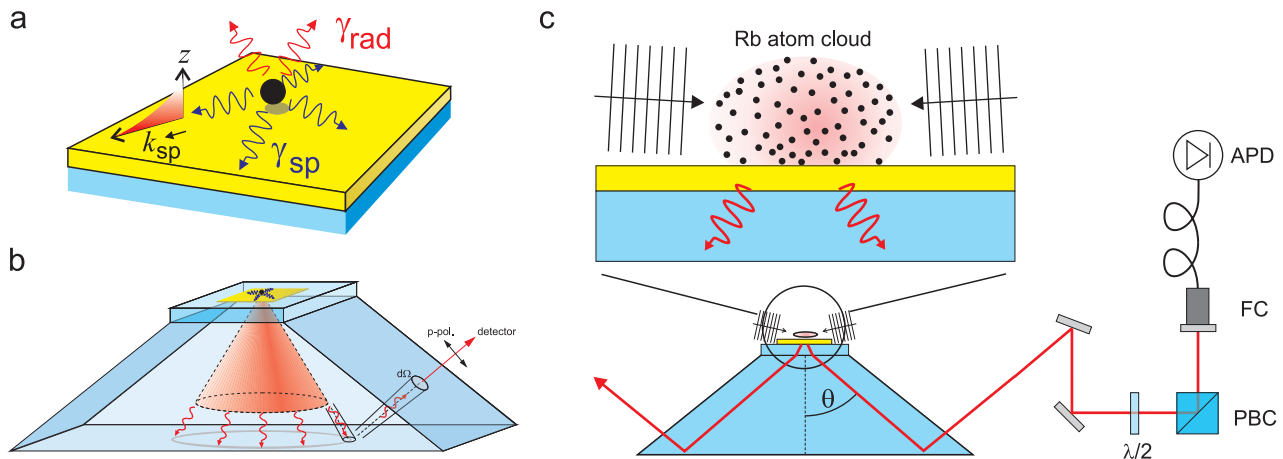


FIG. 1: **Schematic drawing of experimental situation.**

**a** An atom situated close to a metal surface emits photons radiatively with rate  $\gamma_{\text{rad}}$  into free space and nonradiatively with rate  $\gamma_{\text{sp}}$  into surface plasmons propagating on the metal surface with wavenumber  $k_{\text{sp}}$ . **b** Surface plasmons on a thin metal film couple to the far field in the dielectric substrate via leakage radiation. The emitted light field is p-polarized. A detector collects photons under the solid angle  $d\Omega$ . **c** In the experiment a cloud of ultracold Rubidium atoms is positioned very close to a gold film and is illuminated by a laser field. Photons which are emitted into the substrate are collected by an optical fibre coupler (FC) under an adjustable angle  $\theta$  and are detected with an avalanche photo diode (APD) with single photon sensitivity. The polarization of the detected light can be switched between s and p by a  $\lambda/2$  waveplate and a polarizing beam cube (PBC).

coupling single atoms to plasmonic devices [50]. In this Article, we demonstrate direct and cooperative coupling of the fluorescence of cold atoms to surface plasmons propagating on a plane gold surface. The experiment is carried out with the experimental setup described in detail in [50]. An ultracold  $^{87}\text{Rb}$  atom cloud consisting of  $N_{\text{at}} \sim 10^6$  atoms with a temperature of  $T \sim 1 \mu\text{K}$  is trapped in a magnetic trap inside a UHV chamber. By applying external magnetic fields the trapping position is moved towards a glass prism on which a sapphire substrate is attached (Fig. 1). The sapphire substrate carries square fields of gold layers with  $\sim 50 \text{ nm}$  thickness and  $\sim 100 \mu\text{m}$  side length. The atoms are positioned in a variable distance from one of the gold fields where they are illuminated from the side with a  $200 \mu\text{s}$  long laser pulse. The laser intensity is adjusted to the saturation intensity  $I_{\text{sat}} = 1.6 \text{ mW}/\text{cm}^2$  corresponding to the  $D2$ -line of  $^{87}\text{Rb}$ . The incoming light field excites electric dipole oscillations in the atoms which are partially coupled to surface plasmons within the gold layer. The plasmon excitations decay into freely propagating photons [51]. An avalanche photo diode (APD) with single photon detection efficiency measures the number of photons which is emitted under an adjustable angle  $\theta$  into an aperture-limited opening angle of  $\Delta\phi = \Delta\theta = 0.6^\circ$ . Due to Gaussian optics, this corresponds to a detectable spot size on the gold layer with radius  $R_{\text{det}} = 32 \mu\text{m}$ . The detection scheme is sensitive to the polarization of the emitted light. This is crucial for discerning surface plasmon excitations from stray light [52].

Direct coupling between dipolar emitters and surface

plasmons has been theoretically described in the context of nonradiative energy transfer [53, 54]. The theories are based on a single electric dipole  $\vec{d}(t)$  oscillating with frequency  $\omega$  at a position  $\vec{r}_0$ . It generates a radiation field  $\vec{E}_0(\vec{r}, t)$ . The energy decay rate of the dipole is proportional to the product of the dipole moment and the electric field at the position of the dipole,  $\gamma = \frac{1}{2}\omega \cdot \text{Im}[\vec{d} \cdot \vec{E}_0(\vec{r}_0)]$  which, in free-space, results in

the well-known Larmor formula  $\gamma_0 = \frac{\omega^4 |\vec{d}|^2}{3c^3}$  [54]. When the emitter is placed nearby a surface, also the part of the radiation field which is reflected at the boundary will interact with the dipole. This results in a modified decay rate, see Fig. 2 a). Moreover, also the emission pattern is changed. While in free space light can be emitted only radiatively, i.e. the wavenumber of the emitted light field is given by  $k_0 = \omega/c$ , surfaces provide the possibility of nonradiative emission into bound surface waves. Their normal component of the wavevector is purely imaginary, whereas the parallel component has a value larger than that in free space,  $k_{\parallel}^{\text{sf}} > k_0$ , i.e. bound surface waves propagate along the surface. Radiative  $\gamma_{\text{rad}}$  and nonradiative  $\gamma_{\text{nr}}$  contributions to the total decay rate  $\gamma = \gamma_{\text{rad}} + \gamma_{\text{nr}}$  can thus be separated by a Fourier expansion of  $\gamma$  with respect to the dimensionless parameter  $\kappa = k_{\parallel}^{\text{sf}}/k_0$  and integration over the corresponding range  $\kappa \leq 1$  resp.  $\kappa > 1$  [54]. The theoretical results for a single  $^{87}\text{Rb}$  atoms at a distance  $z$  from a gold surface are shown in Fig. 2 a). Here, nonradiative decay is mainly due to coupling to surface plasmon modes, with rate  $\gamma_{\text{sp}}$ . These are collective electron oscillations in the metal surface connected with an electromagnetic wave propagat-

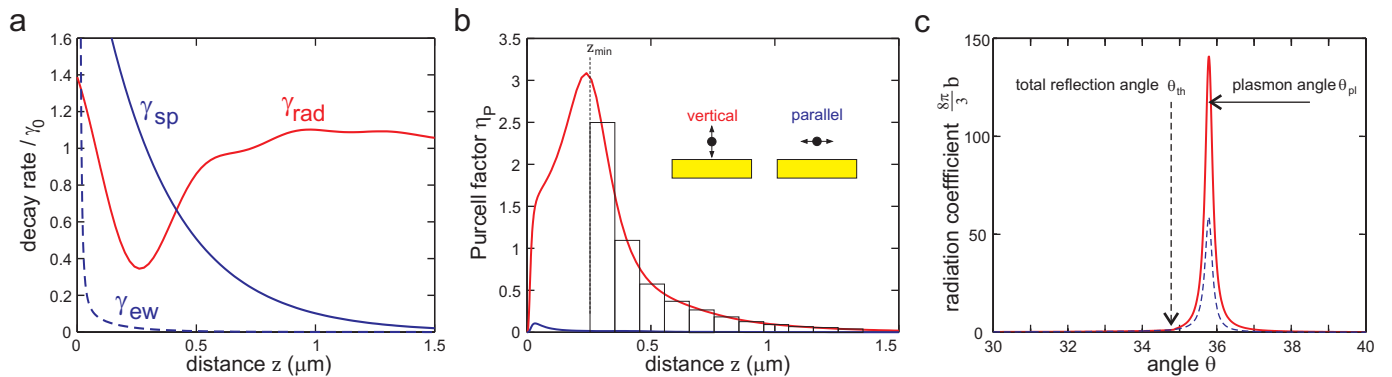


FIG. 2: **Radiation properties of a Rubidium atom at a gold surface.**

**a** Emission rates of a Rubidium atom with orthogonal dipole moment at a distance  $z$  from a gold surface. Red line: Radiative emission into the far field ( $\gamma_{\text{rad}}$ ). Blue solid line: Nonradiative emission into surface plasmons ( $\gamma_{\text{sp}}$ ). Blue dashed line: Nanoradiative emission into evanescent waves ( $\gamma_{\text{ew}}$ ). All rates are normalized to the free space emission rate  $\gamma_0$ . **b** Purcell enhancement factor  $\eta_P = \frac{\gamma_{\text{sp}}}{\gamma_{\text{rad}} + \gamma_{\text{ew}}}$  for a vertical dipole (red line) and a parallel dipole (blue line). Each of the bars at  $z > z_{\text{min}}$  contains approximately 50 atoms. **c** Radiation coefficient for emission into an angle  $\theta$  within the substrate. The solid (dashed) line corresponds to a vertical dipole at a distance of  $z = 250$  (500) nm from a  $d = 50$  nm thick gold layer on top of a sapphire substrate. The dielectric constants at the relevant wavelength of  $\lambda = 780$  nm are  $\epsilon_1 = -22.9 + i \cdot 1.42$  for gold and  $\epsilon_2 = 3.0625$  for sapphire. Obviously, the surface plasmons are coupled into far field radiation in the sapphire substrate with high directionality under the plasmon angle  $\theta_{\text{pl}}$ . The angle of total reflection  $\theta_{\text{th}}$  is that for an interface from sapphire to vacuum.

ing along the surface with wavenumber  $k_{\text{sp}}$ . Decay into other bound modes like evanescent waves with rate  $\gamma_{\text{ew}}$  dominates only for very short distances  $z \lesssim 10$  nm [53]. The efficiency of the direct coupling to surface plasmons is defined via the Purcell factor  $\eta_P = \frac{\gamma_{\text{sp}}}{\gamma_{\text{rad}} + \gamma_{\text{ew}}}$  [10, 55]. Please note, that a large Purcell enhancement  $\eta_P > 1$  is equivalent to the regime of high cooperativity in cqed [56]. As shown in Fig. 2 b a  $^{87}\text{Rb}$  atom which is positioned in a distance range of  $20 \text{ nm} < z < 400 \text{ nm}$  is coupled to plasmons in the gold surface with high cooperativity, if its atomic dipole is oscillating vertically to the surface. In contrast, atoms with parallel oscillating dipoles do not reach the regime of high cooperativity. A peculiarity of atoms as compared to molecules and quantum dots is the fact that the dipolar oscillation axis is not fixed by the orientation of the particle (the polarizability of an atom is radially symmetric), but it is parallel to the electric field of the exciting laser. Thus, the dipolar orientation can, in principle, be adjusted by the polarization of the incident laser pulse. In the present experiment the magnetic offset field of the trapping potential leads to a substantial Faraday rotation of the laser beam polarization while it propagates through the atom cloud. This reduces the number of vertically oscillating dipoles by 1/2 and the plasmon excitation becomes independent of the pump laser polarization. The theory [54] describes also the angular dependence of emitted photons in the far field. The radiation coefficient is given by

$$b(\theta, z) = \frac{3}{8\pi} n_2 \frac{k_x^2}{k_0^2} \left| T_{012}^p \frac{k_{z2}}{k_{z0}} \right|^2 e^{-2\text{Im}(k_{z0})z}, \quad (1)$$

with parallel wavevector  $k_x$ , free space wavevector  $k_0 = 2\pi/\lambda$ , and orthogonal wavevectors  $k_{zj}$  in vacuum ( $j = 0$ )

and sapphire ( $j = 2$ ). The Fresnel field transmission coefficient  $T_{012}^p$  is calculated for the considered three layer system (vacuum / 50 nm gold layer / sapphire substrate) and incident parallel electric field oscillation. The considered dipole is oscillating vertically at a distance  $z$  from the surface. The radiation coefficient is normalized to the free space decay rate  $\gamma_0$  such that the decay rate into a solid angle  $d\Omega$  of the substrate is given by

$$\gamma_2(\theta, d\Omega, z) = \gamma_0 \cdot \int b(\theta, z) d\Omega. \quad (2)$$

As illustrated in Fig. 2 c photons are emitted highly directionally into the substrate under the so-called plasmon angle  $\theta_{\text{pl}}$ . Please note that due to the rotational symmetry of the experimental situation photons are emitted on the surface of a cone, see Fig. 1 b.

The number of detected photons  $N_{\text{det}}$  is plotted in Fig. 3 a versus the trap center distance  $z_0$  from the surface. As the atoms in the trap are moved towards the surface the number of detected photons is increasing. This general behavior is observed for both polarizations ( $s$  and  $p$ ) of the detected light and can be explained by the fact that more photons impinge on the surface when the atoms are closer. Negative values of  $z_0$  correspond to trap centers which are inside the dielectric substrate for which the number of detected photons is decreasing. This decrease is caused by a loss of atoms from the trap as soon as they get into physical contact with the surface. The interesting feature in Fig. 3 a is observed at distances  $0 \lesssim z_0 \lesssim 120 \mu\text{m}$  which are smaller than the radial extension of the cloud such that a sufficient number of atoms can be found at submicron distance from the surface. At such distances an excess of p-polarized photons  $N_{\text{det}}^p$  as

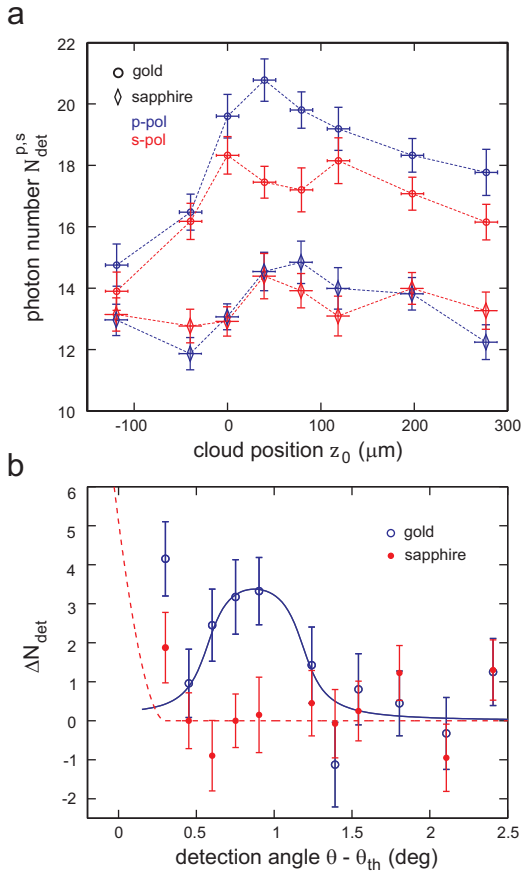


FIG. 3: **Measured photon numbers.**

**a** Number of detected p- and s-polarized photons at an angle of  $\theta - \theta_{\text{th}} = 0.9^\circ$  above the gold surface and above the plain sapphire substrate. The position  $z_0$  is the distance of the cloud center to the surface. **b** The photon number difference  $\Delta N_{\text{det}} = N_{\text{det}}^p - N_{\text{det}}^s$  at a distance of  $z_0 = 41 \mu\text{m}$  has a maximum at the plasmon angle above gold. The solid line is a simulation of nonradiative coupling of the atomic emission to the surface plasmon mode. The only fit parameter in this simulation is a loss factor  $\eta_{\text{add}} = 0.65$  comprising the fibre coupling efficiency of the emitted light and additional losses at optical elements. Above the plain sapphire substrate no maximum is observed. The increase for small angles can be attributed to Fresnel transmission of light through surface roughness.

compared to s-polarized photons  $N_{\text{det}}^p$  is observed above gold. We attribute this excess to the excitation of surface plasmons. Thus, the following analysis concentrates on the observed photon difference  $\Delta N_{\text{det}} = N_{\text{det}}^p - N_{\text{det}}^s$ . In Fig. 3 b the measured angular dependence of  $\Delta N_{\text{det}}$  is shown comparing data which were obtained above the gold layer with data that were taken above the plain sapphire substrate. A maximum of  $\Delta N_{\text{det}}$  is observed at the plasmon angle  $\theta_{\text{pl}}$  above gold. This is caused by the directive emission of surface plasmons into the substrate as calculated theoretically in Fig. 2 c. We simulate this

angular dependence by integration of Eq. 2

$$\Delta N_{\text{sim}} = \int (n_{\text{at}}(\vec{r}) \cdot \gamma_2(\theta, d\Omega, z) \cdot \eta_{\text{ges}} \cdot T_{\text{WW}}) d^3r \quad (3)$$

over the density of the atomic cloud  $n_{\text{at}}(\vec{r}) = N_{\text{at}} (8\pi^3 \sigma_r^4 \sigma_z^2)^{-1/2} e^{-(x^2+y^2)/2\sigma_r^2} e^{-(z-z_0)^2/2\sigma_z^2}$  with cloud width  $\sigma_r = 180 \mu\text{m}$  and  $\sigma_z = 110 \mu\text{m}$  and interaction time  $T_{\text{WW}}$ . The latter is given by the average time it takes for an atom with initial velocity zero to be detuned out of resonance due to radiation pressure. For  $^{87}\text{Rb}$  atoms illuminated with saturation intensity the interaction time is  $T_{\text{WW}} = 84 \mu\text{s}$  [57]. We integrate in the radial direction over the detectable spot size  $R_{\text{det}}$  and in the orthogonal direction from  $z = z_{\text{min}}$  to  $z = \infty$ . The lower integration limit of  $z_{\text{min}} = 260 \text{ nm}$  accounts for the influence of surface potentials and is determined from the fit in Fig. 5. The factor  $\eta_{\text{ges}} = \eta_{\text{qe}} \cdot \eta_{\text{coh}} \cdot \eta_{\text{ort}} \cdot \eta_{\text{add}} = 0.054$  in Eq. 3 includes the quantum efficiency of the single photon counter  $\eta_{\text{qe}} = 0.66$ , the coherent scattering rate factor  $\eta_{\text{coh}} = \gamma_{\text{coh}}/\gamma_0 = 0.25$  at saturation intensity, the fraction of orthogonally oscillating dipoles  $\eta_{\text{ort}} = 0.5$  due to Faraday rotation of the exciting laser field, and a factor  $\eta_{\text{add}} = 0.65$  comprising any additional reduction of the overall detection efficiency, e.g. due to coupling of light into the optical multimode fibre and losses by optical elements. The obtained theoretical curve fits very well to the measured photon numbers in Fig. 3 b. Obviously, our measurement confirms the theoretical prediction. In order to exclude excitation of surface plasmons due to surface roughness, we illuminated the surface with a laser beam without the presence of the atom cloud and determined a photon difference of only  $\Delta N_{\text{det},0} = 0.085$  far below the value shown in Fig. 3 b. Another signature that emphasizes the role of surface plasmons is the fact that above sapphire no peak is observed in  $\Delta N_{\text{det}}$ . There, the number of detected p- and s-polarized photons is equal due to the fact that plasmons do not exist on dielectric surfaces. An additional increase of  $\Delta N_{\text{det}}$  is observed for both substrates (gold and sapphire) at angles very close to the angle of total reflection  $\theta_{\text{th}}$ . This is caused by the fact that part of the detected angle range  $d\theta$  covers angles smaller than  $\theta_{\text{th}}$ . Thus, some of the light which is emitted by the atoms can be transmitted directly through the surface. This behavior is confirmed by a simulation including the angular emission pattern of the atoms and Fresnel transmission into the substrate. The simulation for sapphire is plotted as dashed line in Fig. 3 b and explains the observation qualitatively. The quantitative deviation is attributed to surface roughness which is not taken into account in the simulations and which shifts the simulated curve to larger values of  $\theta$ .

The smoking gun for strong coupling in cqed is the vacuum Rabi splitting in the spectrum [28–35]. This is illustrated in the simulation of the spectral function shown in Fig. 4, where the light power which

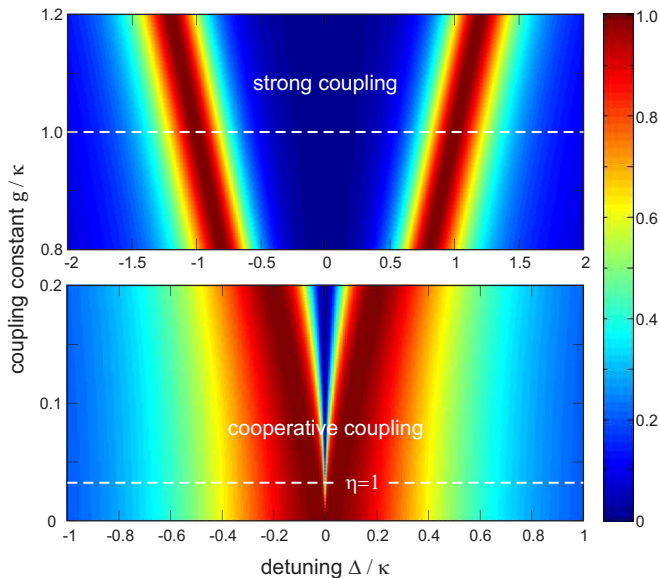


FIG. 4: **Coupling regimes of cqcd.**

The color illustrates the light power radiated by a single atom into an optical cavity as a function of detuning  $\Delta$  from the atomic resonance and of the coupling constant  $g$ . In this simulation the cavity decay rate is chosen to be large (i.e.  $\kappa/\gamma = 250$ ), such that the width of the resonance is given by  $\kappa$ . Each line with constant  $g$  is scaled to its maximum intensity. In the cooperative coupling regime, a narrow dip occurs in the spectrum which gets broader for increasing  $g$ . In the strong coupling regime the width of this dip reaches values larger than  $\kappa$ .

is emitted by an atom into the cavity mode is shown versus the detuning from the atomic resonance for increasing coupling constant  $g$  [56]. In this simulation a ratio of  $\kappa/\gamma = 250$  is chosen in order to illustrate the effect of a large cavity decay rate compared to the atomic decay rate, like in the present experiment. All rates are normalized to  $\gamma$  such that the strong coupling regime is reached for  $g/\kappa \geq 1$ . The cooperative coupling regime  $\eta > 1$  is reached for much smaller values of  $g/\kappa > 0.5(\kappa/\gamma)^{-1/2} = 0.032$ . In this regime the intracavity power has a sharp minimum at  $\Delta = 0$  which is caused by interference of the light field illuminating the atom from outside with the light field which is scattered by the atom into the cavity. In the case of an atom which is positioned close to a metallic surface, the surface plasmon mode plays the role of the cavity mode. For an extended gold surface an effective mode volume can be calculated [58, 59] which depends on the distance of the atom from the surface. For a Rubidium atom with vertically oscillating dipole moment at a distance of  $z_{\min} = 260$  nm from a gold surface the effective mode volume is  $V_{\text{eff}} = 0.442 \mu\text{m}^3$  corresponding to a coupling constant of  $g = \sqrt{3\pi\gamma_0 c^3 / 2\omega_0^2 V_{\text{eff}}} = 2\pi \cdot 6.9$  GHz, with atomic transition frequency  $\omega_0$ . Please note, that this value exceeds those reached hitherto in cold atom experiments with Fabry-Perot cavities ( $g = 2\pi \cdot 215$  MHz) [60]

and photonic crystal cavities ( $g = 2\pi \cdot 300$  MHz) [61] by more than one order of magnitude. The plasmonic decay rate corresponding to the cavity decay rate is given by  $\kappa_{\text{pl}} = 2\pi \cdot v_g/l_{\text{sp}} = 2\pi \cdot 7.45$  THz, with plasmonic group velocity  $v_g$  and plasmonic  $1/e$ -propagation length  $l_{\text{sp}}$  which can both calculated from the plasmonic dispersion relation  $k_{\text{sp}}(\omega)$  [16]. The atomic decay rate in free space is  $\gamma_0 = 2\pi \cdot 6$  MHz. With these number the present experimental situation is far away from the strong coupling regime due to the large plasmonic decay rate  $\kappa_{\text{pl}} \gg g$ , whereas high cooperativity is reached with a maximum value of  $\eta = 4.2$  at  $z_{\min} = 260$  nm distance. This value is similar to the maximum value of  $\eta_{\text{p}} = 3.1$  as shown in Fig. 2 b which underlines the equivalence of Purcell enhancement and high cooperativity.

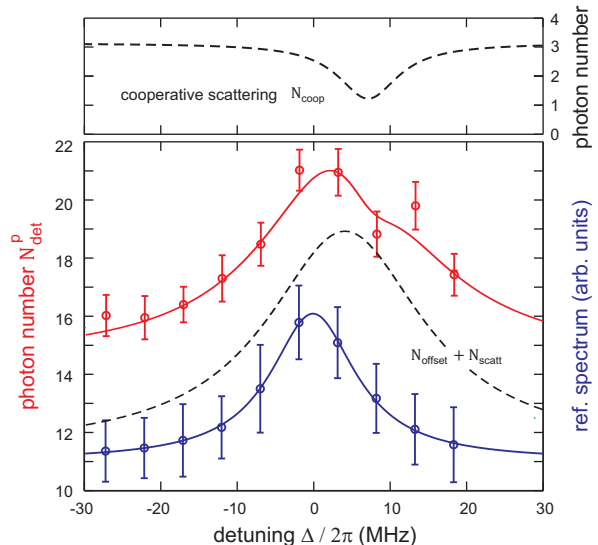


FIG. 5: **Measured spectrum.**

Red circles show the detected photon number  $N_{\text{det}}$  at an emission angle of  $\theta - \theta_{\text{th}} = 0.9^\circ$  and cloud distance  $z_0 = 41 \mu\text{m}$ . The data points are fitted by a model (solid line) including a constant offset  $N_{\text{offset}}$ , a Lorentzian curve with amplitude  $N_{\text{scatt}}$  due to photons scattered by atoms far away from the surface and cooperatively coupled photons  $N_{\text{coop}}$  due to atoms very close to the surface. The natural linewidth  $\gamma$  and the maximum number of cooperatively coupled and detected photons  $N_{\text{coop}}$  were fixed during the fit, with  $N_{\text{coop}} = 3.1$  being determined from Fig. 3. The best fit is reached with a cooperativity parameter of  $\eta_{\text{p}} = 0.6$ . Further parameters of the fit are  $N_{\text{offset}} = 11.4$ , a maximum value of  $N_{\text{scatt}} = 7.6$ , a linewidth of scattered photons  $\gamma_{\text{scatt}} = 2\pi \cdot 28$  MHz, and shifts of the resonance frequencies of  $\delta_{\text{scatt}} = 2\pi \cdot 4.1$  MHz and  $\delta_{\text{coop}} = 2\pi \cdot 7.4$  MHz. For comparison, a reference spectrum (blue circles) was recorded simultaneously by saturation spectroscopy in a Rubidium vapor cell. The reference spectrum is fitted by a Lorentzian function with width  $\gamma_{\text{ref}} = 2\pi \cdot 14$  MHz.

Fig. 5 shows the corresponding spectrum recorded by the APD signal while tuning the laser across the Rubidium resonance. The measured signal is composed of (i) stray light from solid objects, (ii) stray light from atoms

far away from the surface and (iii) cooperatively coupled photons due to atoms close to the surface. These three contributions are modelled by (i) a constant offset, (ii) a Lorentzian line shape and (iii) by a spectral function as shown in Fig. 4, respectively. Cooperative coupling is observed as a dip in the spectrum at  $\Delta/2\pi \sim 8$  MHz. The composed theory curve is fitted to the data resulting in a fitted value for the cooperativity parameter  $\eta_{\text{P}}^{\text{fit}} = 0.6$ . The deviation of the fitted value from the theoretically expected value of  $\eta_{\text{P}} = 3.1$  is caused by the position spread  $\sigma_z$  of the atom cloud in the experiment. Thus, the overall coupling efficiency into surface plasmons is the average over all contributions. The distance dependent weighting function  $\beta(z) = \frac{\gamma_{\text{sp}}}{\gamma_{\text{rad}} + \gamma_{\text{ew}}}$  accounts for this varying contribution. The average Purcell enhancement is thus calculated to be

$$\langle \eta_{\text{P}} \rangle = \frac{\int_{z_{\text{min}}}^{\infty} \beta(z) \cdot \eta_{\text{P}}(z) dz}{\int_0^{\infty} \beta(z) dz} = 0.6, \quad (4)$$

where the lower integration limit  $z_{\text{min}} = 260$  nm is adjusted in order to obtain the experimentally observed value of  $\langle \eta_{\text{P}} \rangle = 0.6$ . The assumption of a lower boundary is motivated by the presence of dispersion forces which attract the atoms to the surface and remove them from the detection volume on a short timescale as compared to the interaction time  $T_{\text{WW}}$ . For comparison, a lower integration limit of  $z_{\text{min}} = 0$  would correspond to a mean value of  $\langle \eta_{\text{P}} \rangle = 1.5$ . The centers of the Lorentzian curve and the spectral function are shifted with respect to a reference spectrum recorded simultaneously. This shift can be explained by the Zeeman-shift due to magnetic trapping fields in the vacuum chamber on the order of few Gauss.

Concluding, we have observed cooperative coupling be-

tween ultracold atoms and surface plasmons. Clouds of cold atoms are positioned in a magnetic trap at the surface of a sapphire substrate which is coated with a thin gold layer. The atoms are illuminated and excited with a laser pulse and, depending on the distance of the atoms from the surface, the atomic excitation decays with high probability into surface plasmons that propagate along the metal surface. The plasmons are detected via photons that are emitted into the substrate. If the cloud is close enough to the surface more p-polarized than s-polarized photons are detected which is a signature of surface plasmons. The number of detected photons and the observed angular dependence of the emitted light fit quantitatively very well to the theoretical prediction with a maximum Purcell enhancement of  $\eta_{\text{P,max}} = 3.1$  and a mean Purcell enhancement of  $\langle \eta_{\text{P}} \rangle = 0.6$ , where the average is taken over the contributions of atoms at different distance from the surface. We show that these values are consistent with the predictions of cavity quantum electrodynamics when the plasmon mode is interpreted as cavity mode. Despite the large intrinsic losses connected with surface plasmons, the cooperative coupling regime is reached because of the extremely large coupling constant of  $g = 2\pi \cdot 6.9$  GHz. This is corroborated by the observation of a dip in the spectrum which is a characteristic feature of high cooperativity. These results demonstrate that hybrid systems consisting of cold atoms and surface plasmons have the potential for photonic devices on the single photon level with coupling constants hitherto unreached in cold atom experiments. Moreover, the cooperative coupling of individual atoms with the surface plasmon mode leads to long-range interactions between different atoms. The emission properties can thus be more complex than for a single atom[62] with quantum correlations arising between the atoms.

- 
- [1] Haroche, S. & Raimond, J.-M. *Exploring the quantum: Atoms, Cavities, Photons*. (Oxford Univ. Press, New York, 2006).
- [2] Imamoglu, A. & Yamamoto, Y. Turnstile device for heralded single photons: coulomb blockade of electron and hole tunneling in quantum confined p-i-n heterojunctions. *Phys. Rev. Lett.* **72**, 210-213 (2011).
- [3] Kim, J., Benson, O., Kan, H. & Yamamoto, Y. A Single-photon turnstile device. *Nature* **397**, 500-503 (1999).
- [4] He, Y.-M. et al. On-demand semiconductor single-photon source with near-unity indistinguishability. *Nature Nanotech.* **8**, 213-217 (2013).
- [5] Englund, D. et al. Controlling the spontaneous emission rate of single quantum in a two-dimensional photonic crystal. *Phys. Rev. Lett.* **95**, 013904 (2005).
- [6] Yamamoto, Y. & Imamoglu, A. *Mesoscopic Quantum Optics*. (Wiley & Sons, 1999).
- [7] Birnbaum, K.M. et al. Photon blockade in an optical cavity with one trapped atom. *Nature* **436**, 87-90 (2005).
- [8] Peyronel, T. et al. Quantum nonlinear optics with single photons enabled by strongly interacting atoms. *Nature* **488**, 57-60 (2012).
- [9] Volz, T. et al. Ultrafast all-optical switching by single photons. *Nature Phot.* **6**, 605-609 (2012).
- [10] Chang, D.E., Sørensen, A.S., Demler, E.A. & Lukin, M.D. A single-photon transistor using nanoscale surface plasmons. *Nature Phys.* **3**, 807 - 812 (2007).
- [11] Neumeier, L., Leib, M. & Hartmann, M.J. et al. Single-Photon Transistor in Circuit Quantum Electrodynamics. *Phys. Rev. Lett.* **111**, 063601 (2013).
- [12] Kimble, H.J. Strong interactions of single atoms and photons in cavity qed. *Physica Scripta T* **76**, 127 (1998).
- [13] Khitrova, G., Gibbs, H.M., Kira, M., Koch, S.W. & Scherer, A. Vacuum Rabi splitting in semiconductors. *Nature Phys.* **2**, 81-90 (2006).
- [14] Benson, O. Assembly of hybrid photonic architectures from nanophotonic constituents. *Nature* **480**, 193-199 (2011).
- [15] Kimble, H.J. Strong interactions of single atoms and photons in cavity qed. *Physica Scripta T* **76**, 127 (1998).

- [16] Barnes, W.L., Dereux, A. & Ebbesen, T.W. Surface plasmon subwavelength optics. *Nature* **424**, 824-830 (2003).
- [17] Gramotnev, D.K. & Bozhevolnyi, S.I. Plasmonics beyond the diffraction limit. *Nature Photon.* **4**, 83-91 (2010).
- [18] Schuller, J.A. et al. Plasmonics for extreme light concentration and manipulation. *Nature Mater.* **9**, 193-204 (2010).
- [19] Weber, W.H. & Eagen, C.F. Energy transfer from an excited dye molecule to the surface plasmons of an adjacent metal. *Opt. Lett.* **4**, 236-238 (1979).
- [20] Pockrand, I. & Brillante, A. Nonradiative Decay Of Excited Molecules Near A Metal Surface. *Chem. Phys. Lett.* **69**, 499-504 (1980).
- [21] Chang, D.E., Sørensen, A.S., Hemmer, P.R. & Lukin, M.D. Quantum Optics with Surface Plasmons. *Phys. Rev. Lett.* **97**, 053002 (2006).
- [22] Tame, M.S., McEnery, K.R., zdemir, S.K., Lee, J., Maier, S.A. & Kim, M.S. Quantum Plasmonics. *Nature Phys.* **9**, 329 - 340 (2013).
- [23] Amos, R.M., & Barnes, W.L. Modification of the spontaneous emission rate of  $\text{Eu}^{3+}$  ions close to a thin metal mirror. *Phys. Rev. B* **55**, 7249-7254 (1997).
- [24] Anger, P., Bharadwaj, P. & Novotny, L. Enhancement and Quenching of Single-Molecule Fluorescence. *Phys. Rev. Lett.* **96**, 113002 (2006).
- [25] Andersen, M.L., Stobbe, S., Sørensen, A.S. & Lodahl, P. Strongly modified plasmons-matter interaction with mesoscopic quantum emitters *Nature Phys.* **7**, 215 - 218 (2010).
- [26] Akimov, A.V. et al. Generation of single optical plasmons in metallic nanowires coupled to quantum dots. *Nature* **450**, 402 - 406 (2007).
- [27] Huck, A., Kumar, S., Shakoor, A. & Andersen, U.L. Controlled Coupling of a Single Nitrogen-Vacancy Center to a Silver Nanowire. *Phys. Rev. Lett.* **106**, 096801 (2011).
- [28] Bellessa, J., Bonnand, C. & Plenet, J.C. Strong coupling between Surface Plasmons and Excitons in an Organic Semiconductor. *Phys. Rev. Lett.* **93**, 036404 (2004).
- [29] Dintinger, J., Klein, S., Bustos, F., Barnes, W.L. & Ebbesen, T.W. Strong coupling between surface plasmon-polaritons and organic molecules in subwavelength hole arrays. *Phys. Rev. B* **71**, 035424 (2005).
- [30] Vasa, P. et al. Coherent Exciton-Surface-Plasmon-Polariton Interaction in Hybrid Metal-Semiconductor Nanostructures. *Phys. Rev. Lett.* **101**, 116801 (2008).
- [31] Hakala, T.K. et al. Vacuum Rabi Splitting and Strong-Coupling Dynamics for Surface-Plasmon Polaritons and Rhodamine 6G Molecules. *Phys. Rev. Lett.* **103**, 053602 (2009).
- [32] Gómez, D.E. , Vernon, K.C., Mulvaney, P. & Davis, T.J. Surface Plasmon Mediated Strong Exciton-Photon Coupling in Semiconductor Nanocrystals. *Nano Lett.* **10**, 274-278 (2010).
- [33] Schwartz, T., Hutchison, J.A., Genet, C. & Ebbesen, T.W. Reversible Switching of Ultrastrong Light-Molecule Coupling. *Phys. Rev. Lett.* **106**, 196405 (2011).
- [34] Aberra Guebrou, S. et al. Coherent Emission from a Disordered Organic Semiconductor Induced by Strong Coupling with Surface Plasmons. *Phys. Rev. Lett.* **108**, 066401 (2012).
- [35] González-Tudela, A., Huidobro, P.A., Martín-Moreno, C. & García-Vidal, F.J. Theory of Strong Coupling between Quantum Emitters and Propagating Surface Plasmons. *Phys. Rev. Lett.* **110**, 126801 (2013).
- [36] Chang, D.E. et al. Trapping and Manipulation of Isolated Atoms Using Nanoscale Plasmonic Structures. *Phys. Rev. Lett.* **103**, 123004 (2009).
- [37] Murphy, B. & Hau, L.V. Electro-Optical Nanotraps for Neutral Atoms. *Phys. Rev. Lett.* **102**, 033003 (2009).
- [38] Gullans, M. et al. Nanoplasmonic Lattices for Ultracold Atoms. *Phys. Rev. Lett.* **109**, 235309 (2012).
- [39] Righini, M., Zelenina, A.S., Girard, C. & Quidant, R. Parallel and selective trapping in a patterned plasmonic landscape. *Nature Phys.* **3**, 477-480 (2007).
- [40] Anderson, M.H., Ensher, J.R., Matthews, M.R., Wieman, C.E. & Cornell, E.A. Observation of Bose-Einstein Condensation in a Dilute Atomic Vapor. *Science* **269**, 198-201 (1995).
- [41] Fortágh, J. & Zimmermann, C. Magnetic microtraps for ultracold atoms. *Rev. Mod. Phys.* **79**, 235-289 (2007).
- [42] Grimm, R., Weidemüller, M. & Ovchinnikov, Y.B. Optical Dipole Traps for Neutral Atoms. *Adv. At. Mol. Opt. Phys.* **42**, 95-170 (2000).
- [43] Wilk, T. et al. Entanglement of Two Individual Neutral Atoms Using Rydberg Blockade. *Phys. Rev. Lett.* **104**, 010502 (2010).
- [44] Juliá-Díaz, B., Graß, T., Dutta, O., Chang, D.E. & Lewenstein, M. Engineering p-wave interactions in ultracold atoms using nanoplasmonic traps. *Nature Commun.* **4**, 2046 (2013).
- [45] Chang, D.E., Cirac, J.I. & Kimble, H.J. Self-Organization of Atoms along a Nanophotonic Waveguide. *Phys. Rev. Lett.* **110**, 113606 (2013).
- [46] Thompson, J.D. et al. Coupling a Single Trapped Atom to a Nanoscale Optical Cavity. *Science* **340**, 1202-1205 (2013).
- [47] Esslinger, T., Weidemüller, M., Hemmerich, A. & Hänsch, T.W. Surface-plasmon mirror for atoms. *Opt. Lett.* **18**, 450-452 (1993).
- [48] Feron, S. et al. Reflection of metastable neon atoms by a surface plasmon wave. *Opt. Comm.* **102**, 83-88 (1993).
- [49] Schneble, D., Hasuo, M., Anker, T., Pfau, T. & Mlynek, J. Detection of cold metastable atoms at a surface. *Rev. Sci. Instr.* **74**, 2685-2689 (2003).
- [50] Stehle, C. et al. Plasmonically tailored micropotentials for ultracold atoms. *Nature Photon.* **5**, 494-498 (2011).
- [51] Hohenau, A. et al. Surface plasmon leakage radiation microscopy at the diffraction limit. *Opt. Exp.* **19**, 25749-25762 (2011).
- [52] Raether, H. *Surface Plasmons on Smooth and Rough Surfaces and on Gratings* (Springer-Verlag, Berlin, 1988).
- [53] Chance, R.R., Prock, A. & Silbey, R. Molecular Fluorescence And Energy Transfer Near Interfaces. *Adv. Chem. Phys.* **37**, 1-65 (1978).
- [54] Sipe, J.E. The Dipole Antenna Problem In Surface Physics: A New Approach. *Surf. Science* **105**, 489-504 (1981).
- [55] Chang, D.E., Sørensen, A.S., Hemmer, P.R. & Lukin, M.D. Strong coupling of single emitters to surface plasmons. *Phys. Rev. B* **76**, 035420 (2007).
- [56] Tanji-Suzuki, H. et al. Interaction between Atomic Ensembles and Optical Resonators: Classical description. *Adv. At. Mol. Opt. Phys.* **60**, 201 (2011).
- [57] Cohen-Tannoudji, C., Dupont-Roc, J. & Grynberg, G. *Atom-photon interactions, basic processes and applications* (Wiley, New York, 1992).
- [58] Archambault, A., Teperik, T.V. , Marquier, F. & Greffet, J.J. Surface plasmon Fourier optics. *Phys. Rev. B* **79**,

- 195414 (2009).
- [59] Archambault, A., Marquier, F., Greffet, J.J. & Arnold, C. Quantum theory of spontaneous and stimulated emission of surface plasmons. *Phys. Rev. B* **82**, 035411 (2010).
- [60] Gehr, R. et al. Cavity-Based Single Atom Preparation and High-Fidelity Hyperfine State Readout. *Phys. Rev. Lett* **104**, 203602 (2010).
- [61] Thompson, J.D. et al. Coupling a Single Trapped Atom to a Nanoscale Optical Cavity. *Science*.1237125 (2013).
- [62] Choquette, J.J., Marzlin, K.-P. & Sanders, B.C. Superradiance, subradiance, and suppressed superradiance of dipoles near a metal interface *Phys. Rev. A* **82**, 023827

(2010).

## I. ACKNOWLEDGEMENT

C.Z. gratefully acknowledges financial support by the DFG. C.S. was supported by Carl-Zeiss Stiftung Baden-Württemberg. S. S. is indebted to the Baden-Württemberg Stiftung for the financial support of this research project by the Eliteprogramm for Postdocs.